CHEMISTRY OF MATERIALS
Article

Chem. Mater. **2010,** *22,* 2427–2433 2427
DOI:10.1021/cm9009942

Effects of Lithium Ions on Dye-Sensitized ZnO Aggregate Solar Cells

Qifeng Zhang,[†] Christopher S. Dandeneau,[†] Stephanie Candelaria,[†] Dawei Liu,[†] Betzaida B. Garcia,[†] Xiaoyuan Zhou,[†] Yoon-Ha Jeong,[‡] and Guozhong Cao*,[†]

[†]*Department of Materials Science and Engineering, University of Washington, Seattle, Washington 98195, and* [‡]*National Center for Nanomaterials Technology (NCNT), Pohang University of Science and Technology, Pohang, South Korea*

Received April 9, 2009. Revised Manuscript Received February 2, 2010

We report on the synthesis of ZnO nanocrystallite aggregates in the presence of lithium ions and films consisting of these aggregates for dye-sensitized solar cell applications. A maximum overall conversion efficiency of 6.1% has been achieved with these films. This value is much higher than the 4.0% obtained for the films that are comprised of ZnO aggregates synthesized in the absence of lithium ions. The lithium ions were found to have an influence on the growth and assembly of ZnO nanocrystallites, leading to an increase in the nanocrystallite size and a polydisperse distribution in the size of the aggregates. The increase in the nanocrystallite size is due to a lithium-induced increase in the diffusivity of interstitial zinc atoms, which leads to an improvement in the crystallinity. This, in turn, yields an oxygen-enriched ZnO surface, which acts to suppress the dissolution of zinc atoms at the ZnO surface in the case of an acidic dye. As such, the formation of a Zn^{2+}/dye complex is avoided. This collaborates with an increase in the pore size of the aggregates in view of the increase in the nanocrystallite size, allowing dye molecules to undergo a thorough infiltration into the photoelectrode film so as to be more adsorbed. The polydisperse size distribution of the aggregates is believed to favor light scattering so that the traveling distance of light within the photoelectrode film can be significantly extended. Both the improved dye adsorption and the enhanced light scattering serve to increase the light-harvesting efficiency of the photoelectrode and, thus, promote the overall conversion efficiency of solar cells.

I. Introduction

The worldwide demand for energy has increased with the consumption of oil reserves. This has spurred the development of new energy sources that are cost-effective and environmentally friendly. Solar radiation is arguably an ideal source of energy. The conversion from solar radiation to electricity may be fulfilled by solar cells, a class of electrical devices that, through the photovoltaic effect, generate and then separate photogenerated carriers. For several decades, crystalline silicon and compound semiconductor thin films have been developed for solar cell use. However, such devices still possess the disadvantage of high production cost.[1] To address this issue, many studies in the past 2 decades have been focused on the development of dye-sensitized solar cells (DSCs), which feature low cost but relatively high conversion efficiency.[2−4]

Many wide-band-gap oxides such as TiO_2,[5] ZnO,[6] SnO_2,[7] and Nb_2O_5[8] have been investigated as photoelectrode materials in DSCs. In addition, various nanostructures such as nanoparticles, nanowires/nanorods, and nanotubes serve to offer a large surface area for dye adsorption and/or a direct pathway for electron transport.[9,10] To date, a maximum solar-to-electricity conversion efficiency of about 11% was obtained on TiO_2 nanocrystalline films, which feature a highly porous structure with a large specific surface area for dye adsorption.[11,12] Besides the desired structure of the photoelectrode film, the achievement of

*To whom correspondence should be addressed. Fax: 206-543-3100. E-mail: gzcao@u.washtington.edu.

(1) Liu, J.; Cao, G. Z.; Yang, Z.; Wang, D.; Dubois, D.; Zhou, X.; Graff, G. L.; Pederson, L. R.; Zhang, J.-G. Oriented nanostructures for energy conversion and storage. *ChemSusChem* **2008**, *1*(8−9), 22.
(2) Oregan, B.; Gratzel, M. A low-cost, high-efficiency solar-cell based on dye-sensitized colloidal TiO_2 films. *Nature* **1991**, *353*(6346), 737–740.
(3) Gratzel, M. Dye-sensitized solar cells. *J. Photochem. Photobiol., C* **2003**, *4*(2), 145–153.
(4) Zhang, Q. F.; Dandeneau, C. S.; Zhou, X. Y.; Cao, G. Z. ZnO nanostructures for dye-sensitized solar cells. *Adv. Mater.* **2009**, *21* (41), 4087–4108.
(5) Gratzel, M. Sol-gel processed TiO_2 films for photovoltaic applications. *J. Sol−Gel Sci. Technol.* **2001**, *22*(1−2), 7–13.
(6) Suri, P.; Panwar, M.; Mehra, R. M. *Photovoltaic performance of dye-sensitized ZnO solar cell based on Eosin-Y photosensitizer*; Materials Science: Wroclaw, Poland, 2007; pp 137−144.
(7) Bergeron, B. V.; Marton, A.; Oskam, G.; Meyer, G. J. Dye-sensitized SnO_2 electrodes with iodide and pseudohalide redox mediators. *J. Phys. Chem. B* **2005**, *109*(2), 937–943.
(8) Sayama, K.; Sugihara, H.; Arakawa, H. Photoelectrochemical properties of a porous Nb_2O_5 electrode sensitized by a ruthenium dye. *Chem. Mater.* **1998**, *10*(12), 3825–3832.
(9) Hamann, T. W.; Jensen, R. A.; Martinson, A. B. F.; Van Ryswyk, H.; Hupp, J. T. Advancing beyond current generation dye-sensitized solar cells. *Energy Environ. Sci.* **2008**, *1*(1), 66–78.
(10) Law, M.; Greene, L. E.; Johnson, J. C.; Saykally, R.; Yang, P. D. Nanowire dye-sensitized solar cells. *Nat. Mater.* **2005**, *4*(6), 455–459.
(11) Kroon, J. M.; Bakker, N. J.; Smit, H. J. P.; Liska, P.; Thampi, K. R.; Wang, P.; Zakeeruddin, S. M.; Gratzel, M.; Hinsch, A.; Hore, S.; Wurfel, U.; Sastrawan, R.; Durrant, J. R.; Palomares, E.; Pettersson, H.; Gruszecki, T.; Walter, J.; Skupien, K.; Tulloch, G. E. Nanocrystalline dye-sensitized solar cells having maximum performance. *Prog. Photovoltaics* **2007**, *15*(1), 1–18.
(12) Gratzel, M. Solar energy conversion by dye-sensitized photovoltaic cells. *Inorg. Chem.* **2005**, *44*(20), 6841–6851.

Published on Web 03/31/2010

such a high conversion efficiency for DSCs is also attributed to the use of ruthenium-based dyes as the photosensitizer. These dyes, known as N3, N719, or black dye, are very efficient in capturing most of the photons with wavelengths in the visible region. More importantly, the photogenerated electrons in these dyes have a long excited-state lifetime and can therefore effectively inject from the dye molecules to the semiconductor (~100 fs) before radiative or nonradiative recombination occurs (~15 ns).[9]

ZnO, one of the most common II−VI semiconductors, has been regarded as a promising alternative to TiO_2 in DSCs.[4] As a photoelectrode material, ZnO possesses a wide energy band gap similar to that of TiO_2. The use of ZnO in DSCs is thought to be advantageous with regards to crystallization and electrical conduction. ZnO can be easily fabricated into various nanostructures. Furthermore, ZnO possesses an electron mobility of 115−155 $cm^2\ V^{-1}\ s^{-1}$, which is 7 orders of magnitude higher than ~10^{-5} $cm^2\ V^{-1}\ s^{-1}$ for TiO_2.[13,14] Many studies have focused on the application of ZnO in DSCs. However, the reported conversion efficiencies are still relatively low when compared with those of DSCs with TiO_2 photoelectrodes. Conversion efficiencies of 1.5−5% for ZnO nanocrystalline films,[15−18] 0.3−4.7% for ZnO nanowires,[10,19−21] 1.6−2.3% for ZnO nanotubes,[22,23] and 0.23−5.08% for ZnO nanoporous films[24,25] have been previously attained. In addition to the insufficient specific surface area obtainable for ZnO films, the poor photovoltaic performance observed in ZnO-based DSCs has been mainly caused by the instability of ZnO in a ruthenium-based dye solution. This instability results in the formation of an inactive Zn^{2+}/dye complex layer on the ZnO surface and, therefore, lowers the injection efficiency of electrons from the dye molecules to the ZnO semiconductor.[26,27]

In our previous work, we reported conversion efficiencies above 3.5% using ZnO films with a hierarchical structure. These films are comprised of numerous spherical aggregates consisting of nanosized crystallites.[28,29] It has been demonstrated that the ZnO aggregates possess a submicrometer size, which is comparable to the wavelengths of incident light. Therefore, light scattering can be generated within the photoelectrode film. As a result, the traveling distance of light is significantly extended by several hundred times, leading to an increase in the light-harvesting efficiency (LHE) of the photoelectrode. We have also indicated that the average size of the aggregates and their size distribution can be adjusted either by using a stock solution that contains ZnO nanoparticles or by changing the heating rate during the synthesis of the ZnO aggregates. In comparison with films that consist of ZnO aggregates with a monodisperse size distribution, it was found that films with polydisperse aggregates could form a more disordered structure and, thus, cause an increase in light scattering within the photoelectrode film.[30] In this paper, we report a novel route to synthesizing polydisperse ZnO aggregates using lithium ions to mediate the growth of the aggregates. With photoelectrode films containing as-fabricated ZnO aggregates, a maximum conversion efficiency of 6.1% has been achieved. It will be shown that the use of lithium ions may induce the growth of ZnO nanocrystallites and, meanwhile, significantly improve the surface stability of ZnO in an acidic dye. The high conversion efficiency is attributed to both the polydisperse size distribution of the aggregates, which contributes to the light scattering, and the improved surface stability of ZnO, which enables the dye molecules to adsorb on ZnO in a monolayer.

II. Experimental Section

The method used for fabricating ZnO aggregates via a hydrolysis−condensation reaction is similar to that described elsewhere.[31] However, in this study, a lithium salt is employed to

(13) Kaidashev, E. M.; Lorenz, M.; von Wenckstern, H.; Rahm, A.; Semmelhack, H. C.; Han, K. H.; Benndorf, G.; Bundesmann, C.; Hochmuth, H.; Grundmann, M. High electron mobility of epitaxial ZnO thin films on c-plane sapphire grown by multistep pulsed-laser deposition. *Appl. Phys. Lett.* **2003**, *82*(22), 3901–3903.

(14) Dittrich, T.; Lebedev, E. A.; Weidmann, J. Electron drift mobility in porous TiO_2 (anatase). *Phys. Status Solidi A* **1998**, *165*(2), R5–R6.

(15) Lee, W. J.; Suzuki, A.; Imaeda, K.; Okada, H.; Wakahara, A.; Yoshida, A. Fabrication and characterization of Eosin-Y-sensitized ZnO solar cell. *Jpn. J. Appl. Phys., Part 1* **2004**, *43*(1), 152–155.

(16) Otsuka, A.; Funabiki, K.; Sugiyama, N.; Yoshida, T. Dye sensitization of ZnO by unsymmetrical squaraine dyes suppressing aggregation. *Chem. Lett.* **2006**, *35*(6), 666–667.

(17) Zeng, L. Y.; Dai, S. Y.; Xu, W. W.; Wang, K. J. Dye-sensitized solar cells based on ZnO films. *Plasma Sci. Technol.* **2006**, *8*(2), 172–175.

(18) Keis, K.; Magnusson, E.; Lindstrom, H.; Lindquist, S. E.; Hagfeldt, A. A 5% efficient photoelectrochemical solar cell based on nanostructured ZnO electrodes. *Sol. Energy Mater. Sol. Cells* **2002**, *73*(1), 51–58.

(19) Baxter, J. B.; Aydil, E. S. Nanowire-based dye-sensitized solar cells. *Appl. Phys. Lett.* **2005**, *86*(5), 053114.

(20) Baxter, J. B.; Walker, A. M.; van Ommering, K.; Aydil, E. S. Synthesis and characterization of ZnO nanowires and their integration into dye-sensitized solar cells. *Nanotechnology* **2006**, *17* (11), S304–S312.

(21) Rao, A. R.; Dutta, V. Achievement of 4.7% conversion efficiency in ZnO dye-sensitized solar cells fabricated by spray deposition using hydrothermally synthesized nanoparticles. *Nanotechnology* **2008**, *19*, 44.

(22) Martinson, A. B. F.; Elam, J. W.; Hupp, J. T.; Pellin, M. J. ZnO nanotube based dye-sensitized solar cells ZnO nanotube based dye-sensitized solar cells. *Nano Lett.* **2007**, *7*(8), 2183–2187.

(23) Guo, M.; Diao, P.; Cai, S. M. Photoelectrochemical properties of highly oriented ZnO nanotube array films on ITO substrates. *Chin. Chem. Lett.* **2004**, *15*(9), 1113–1116.

(24) Nonomura, K.; Yoshida, T.; Schlettwein, D.; Minoura, H. One-step electrochemical synthesis of ZnO/Ru(dcbpy)(2)(NCS)(2) hybrid thin films and their photoelectrochemical properties. *Electrochim. Acta* **2003**, *48*(20−22), 3071–3078.

(25) Chen, Z. G.; Tang, Y. W.; Zhang, L. S.; Luo, L. J. Electrodeposited nanoporous ZnO films exhibiting enhanced performance in dye-sensitized solar cells. *Electrochim. Acta* **2006**, *51*(26), 5870–5875.

(26) Keis, K.; Lindgren, J.; Lindquist, S. E.; Hagfeldt, A. Studies of the adsorption process of Ru complexes in nanoporous ZnO electrodes. *Langmuir* **2000**, *16*(10), 4688–4694.

(27) Horiuchi, H.; Katoh, R.; Hara, K.; Yanagida, M.; Murata, S.; Arakawa, H.; Tachiya, M. Electron injection efficiency from excited N3 into nanocrystalline ZnO films: Effect of (N3-Zn^{2+}) aggregate formation. *J. Phys. Chem. B* **2003**, *107*(11), 2570–2574.

(28) Chou, T. P.; Zhang, Q. F.; Fryxell, G. E.; Cao, G. Z. Hierarchically structured ZnO film for dye-sensitized solar cells with enhanced energy conversion efficiency. *Adv. Mater.* **2007**, *19*(18), 2588–2592.

(29) Zhang, Q. F.; Chou, T. R.; Russo, B.; Jenekhe, S. A.; Cao, G. Z. Aggregation of ZnO nanocrystallites for high conversion efficiency in dye-sensitized solar cells. *Angew. Chem., Int. Ed.* **2008**, *47*(13), 2402–2406.

(30) Zhang, Q. F.; Chou, T. P.; Russo, B.; Jenekhe, S. A.; Cao, G. Polydisperse aggregates of ZnO nanocrystallites: A method for energy-conversion-efficiency enhancement in dye-sensitized solar cells. *Adv. Funct. Mater.* **2008**, *18*(11), 1654–1660.

(31) Jezequel, D.; Guenot, J.; Jouini, N.; Fievet, F. Submicrometer zinc-oxide particles—elaboration in polyol medium and morphological-characteristics. *J. Mater. Res.* **1995**, *10*(1), 77–83.

mediate the growth of ZnO aggregates. For a typical fabrication process, 0.1 M zinc acetate dihydrate ($ZnAc\cdot 2H_2O$) and 0.01 M lithium salt (e.g., $LiAc\cdot 2H_2O$) were added to diethylene glycol, and the mixture was heated to 160 °C at a rate of 5 °C min^{-1}. The reaction solution became transparent when the temperature reached 130 °C and gradually evolved into a white, cloudy colloid at a temperature of 160 °C. The solution was kept at 160 °C for about 2 h in order to allow for the necessary chemical reactions to occur. The colloid was then concentrated by a sequential treatment of centrifugation (at 6000 rpm for 20 min), removal of the supernatant, and several redispersals of the precipitate in ethanol. The precipitate of ZnO aggregates was finally dispersed in ethanol with a concentration of approximately 0.5 M and then ultrasonicated for about 10 min until a colloidal suspension solution was obtained.

The photoelectrode films, denoted as "Li-ZnO", were prepared through drop-casting of the suspension solution of ZnO aggregates onto fluorine-doped tin oxide glass substrates. The film thickness was about 10 μm and was controlled by adjustment of the amount of suspension solution added upon the glass substrate. Once the films were dry, they were annealed at 350 °C for 1 h in air in order to remove any residual solvent and organic chemicals on the ZnO surface. For the purpose of comparison, films consisting of ZnO aggregates synthesized with no lithium salt, denoted as "pure-ZnO", were also prepared with the same fabrication process. All Li-ZnO and pure-ZnO films were sensitized in $Ru(dcbpy)_2(NCS)_2$ (N3) dye with a concentration of 5×10^{-4} M in ethanol for 20−30 min. The solar cell performance was characterized by recording the photocurrent−voltage behavior while the photoelectrodes were irradiated by AM 1.5 simulated sunlight with a power density of 100 mW cm^{-2}. The electrolyte used contained 0.5 M tetrabutylammonium iodide, 0.1 M lithium iodide, 0.1 M iodine, and 0.5 M 4-*tert*-butylpyridine in acetonitrile.

The film morphology and structure were characterized by scanning electron microscopy (SEM) and X-ray diffraction (XRD). The size distributions of the aggregates were measured with a particle size analyzer (Saturn DigiSizer 5200; Micromeritics Instrument Corp., Norcross, GA), while the aggregates were dispersed in deionized water containing sodium hexametaphosphate $[(NaPO_3)_6]$ as a surfactant; the beam obscuration was set to 10%. An UV/visible spectrometer (Lambda 900; PerkinElmer, Waltham, MA) and a photonic multichannel analyzer equipped with an integrating sphere (A10104-01; Hamamatsu Photonics K.K., Hamamatsu, Japan) were employed for analysis of the optical absorption properties of the ZnO aggregate films. The porosity of the ZnO aggregates was analyzed with a surface area and pore size analyzer (NOVA 4200e; Quantachrome Instruments, Boynton Beach, FL). Measurements of the ζ potential were carried out through the use of a ζ potential analyzer (ZetaPALS; Brookhaven Instruments Ltd., Worcestershire, U.K.) operating under a current of 1.2 mA and an electric field of 14.3 V cm^{-1}.

III. Results and Discussion

Figure 1 shows the typical photovoltaic behavior of ZnO films consisting of aggregates synthesized in the presence and absence of lithium ions. These two types of films display similar open-circuit voltages (V_{OC}) in the range of 640−660 mV and fill factors (FFs) of 0.44−0.48. However, they differ in short-circuit photocurrent densities (I_{SC}), i.e., 13 mA cm^{-2} for pure-ZnO and 21 mA cm^{-2} for Li-ZnO. The larger photocurrent density leads to higher conversion efficiency. The efficiency of the Li-ZnO film reached 6.1%, while a value of 4.0% was attained for the pure-ZnO film.

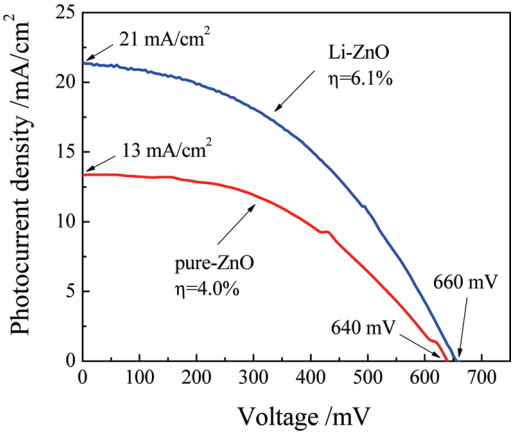

Figure 1. Photovoltaic behavior of ZnO films consisting of aggregates synthesized in the presence (denoted as "Li-ZnO") and absence (denoted as "pure-ZnO") of a lithium salt.

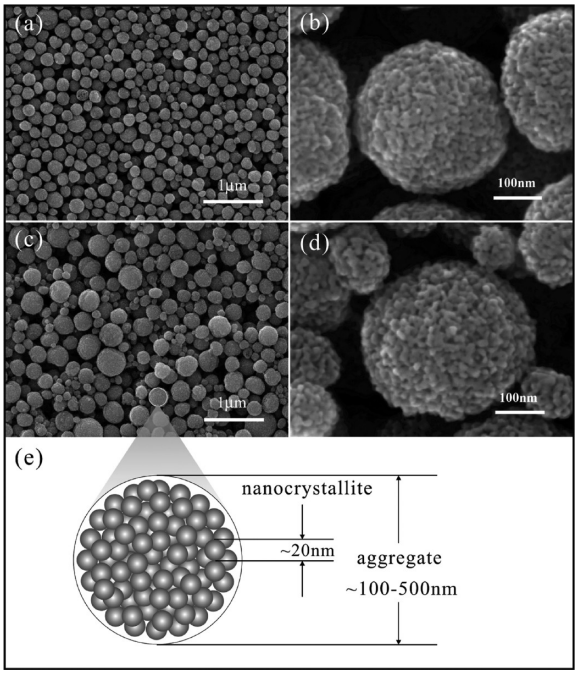

Figure 2. Morphology and structure of ZnO aggregate films. (a and b) SEM images with different magnifications for the pure-ZnO film. (c and d) SEM images for the Li-ZnO film. (e) Drawing to illustrate the hierarchical structure of the aggregates consisting of ZnO nanocrystallites.

Such a ~53% enhancement in the conversion efficiency likely suggests that the use of lithium ions during the ZnO aggregate synthesis may have a positive influence on the solar cell performance by affecting either the morphology, structure, or surface chemistry of the aggregates as well as the photoelectrode film.

Shown in Figure 2 are the SEM images of films that consist of ZnO aggregates synthesized in the absence and presence of lithium ions. It can be seen that both of these films present a hierarchical structure assembled by submicrometer-sized aggregates consisting of nanosized crystallites. These nanocrystallites interconnect and form mesopores inside the aggregates, providing the films with a high porosity.[29] For pure-ZnO and Li-ZnO, some crucial differences can be observed from the SEM images. Specifically, under low

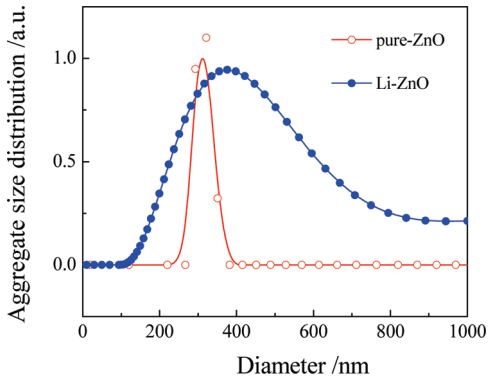

Figure 3. Size distributions of Li-ZnO and pure-ZnO aggregates.

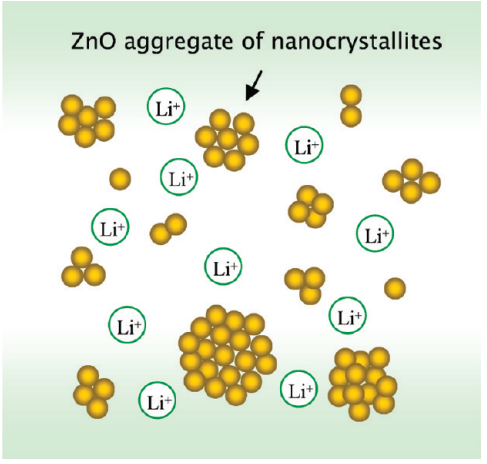

Figure 4. Schematic showing the growth of ZnO aggregates mediated by lithium ions.

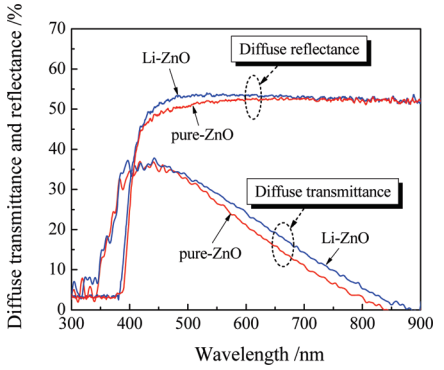

Figure 5. Diffuse-transmittance and -reflectance spectra of the Li-ZnO and pure-ZnO films.

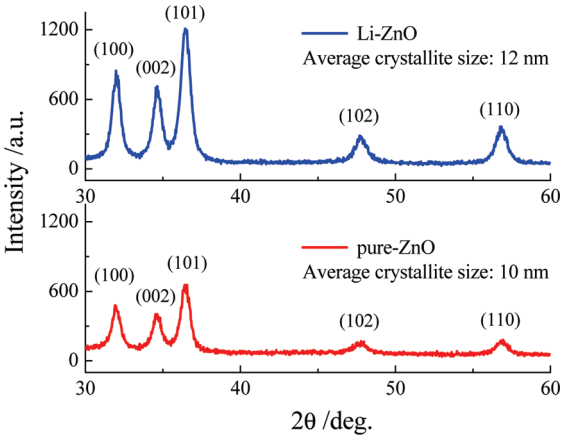

Figure 6. XRD patterns of Li-ZnO and pure-ZnO films, revealing the difference in the nanocrystallite size.

magnification (Figure 2a,c), the pure-ZnO film is comprised of aggregates with a monodisperse size distribution, whereas the Li-ZnO film exhibits a broad distribution of the aggregate size from several tens to several hundreds of nanometers. This is in good agreement with the size distribution measurement of pure-ZnO and Li-ZnO aggregates, as shown in Figure 3.

The polydisperse size distribution of ZnO aggregates synthesized in the presence of a lithium salt reflects the important influence of lithium ions on the growth of ZnO aggregates. As shown in the schematic of Figure 4, it is possible that these lithium ions adsorb on the ZnO surface so as to mediate the agglomeration of ZnO nanocrystallites. Such a polydisperse size distribution of ZnO aggregates has been thought to be beneficial to effective light scattering and, thus, the light traveling distance within the photoelectrode film is significantly extended. This would result in an increase in the LHE of the photoelectrode as well as the conversion efficiency of the solar cell.[32,33] Shown in Figure 5 are the diffuse-transmittance and -reflectance spectra of the pure-ZnO and Li-ZnO aggregate films. The spectra provide definitive evidence of the existence of light scattering for both films in the visible region. The more intensive diffuse transmittance and reflectance of the Li-ZnO aggregate film demonstrate that the light scattering is more effective because of the polydispersity of the aggregate size.

These samples were also characterized through X-ray photoelectron spectroscopy (XPS; see the Supporting Information). However, no detectable difference could be found in the XPS spectra for the pure-ZnO and Li-ZnO films, indicating that these two films are identical with regards to their chemical composition.[34] In other words, it excludes the possibility that lithium exists in ZnO as a dopant or forms a composite with ZnO. However, as stated earlier, we are using the term "Li-ZnO" in this paper to represent the ZnO aggregates synthesized in the presence of lithium ions.

In the high-magnification SEM images shown in Figure 2b,d, a difference in the surface roughness of the aggregates can be observed. The Li-ZnO aggregates present a surface that is coarser than that of pure-ZnO. Such a difference in the surface roughness of pure-ZnO and Li-ZnO aggregates can be ascribed to the difference in the nanocrystallite size. This conclusion is confirmed by the XRD patterns, shown in Figure 6, in which the peak intensity of Li-ZnO is almost twice as strong as that of pure-ZnO, revealing a difference in the crystallinity of

(32) Chiba, Y.; Islam, A.; Komiya, R.; Koide, N.; Han, L. Y. Conversion efficiency of 10.8% by a dye-sensitized solar cell using a TiO_2 electrode with high haze. *Appl. Phys. Lett.* **2006**, *88*(22), 223505.
(33) Chen, D. H.; Huang, F. Z.; Cheng, Y. B.; Caruso, R. A. Mesoporous Anatase TiO_2 Beads with High Surface Areas and Controllable Pore Sizes: A Superior Candidate for High-Performance Dye-Sensitized Solar Cells. *Adv. Mater.* **2009**, *21*(21), 2206–2210.

(34) See the Supporting Information.

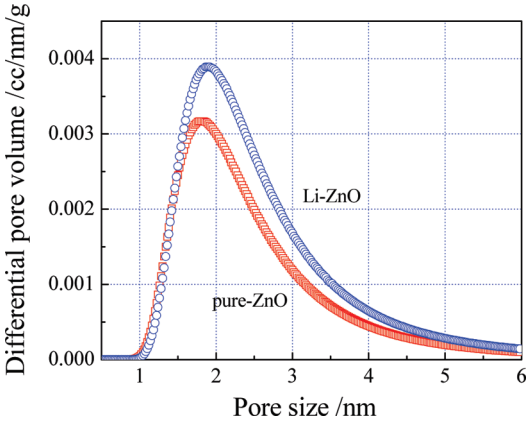

Figure 7. Pore size distribution of pure-ZnO and Li-ZnO aggregates.

these two films. Through the use of Scherrer's equation, it was estimated that the average crystallite sizes are 12 nm for Li-ZnO and 10 nm for pure ZnO.

The difference in the nanocrystallite size likely suggests that, aside from the influence on the growth of aggregates resulting in the polydisperse size distribution, the lithium ions also play a role in promoting the crystallization of ZnO nanocrystallites. A possible explanation is that ZnO is usually an n-type semiconductor with the native defects of oxygen vacancies and zinc interstitials; the interstitial zinc atoms are proven to be determinant in the growth of crystal grains. Lithium ions have a radius of 0.060 nm, smaller than that of 0.074 nm for Zn^{2+}. Therefore, the lithium ions may intercalate into ZnO and enable the interstitial zinc atoms to have a high diffusivity. This, in turn, causes an increase in the concentration of the zinc atoms and, thus, promotes the growth of crystalline ZnO grains.[35−37] In DSCs, the improved crystallinity would be favorable in reducing the energy loss of electrons traveling in the semiconductor photoelectrode film. An increase in the crystallite size may, in theory, cause a slight decrease in the specific surface area of the photoelectrode film. However, in the case of a hierarchical film with aggregates consisting of nanocrystallites, the larger-sized nanocrystallites may result in a porous structure with increased pore sizes. The results of the pore size distribution measurements for pure-ZnO and Li-ZnO aggregates are shown in Figure 7. A difference in the porosity of these two samples is observed; Li-ZnO possesses an average pore size slightly larger than that of pure-ZnO. Such an increase in the pore size would ameliorate the dye infiltration process within the film during sensitization and, thus, shorten the sensitization time so as to prevent the formation of a Zn^{2+}/dye complex. It is also believed that an increase in the pore size could be advantageous toward promoting electrolyte diffusion when the film is used in a DSC configuration under operating conditions.

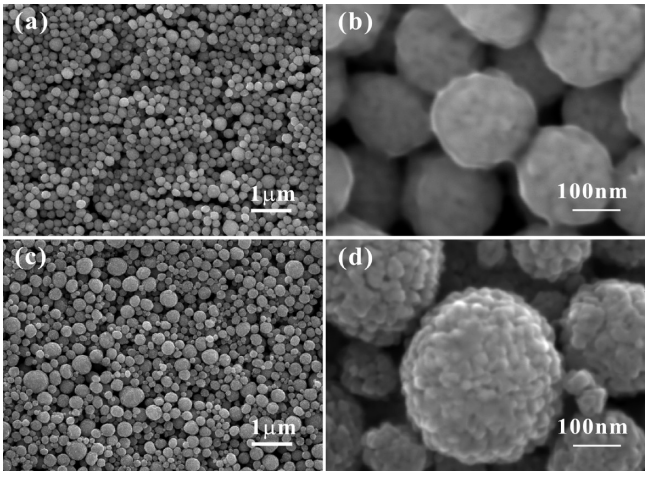

Figure 8. SEM images of ZnO aggregate films after dye sensitization: (a and b) pure-ZnO; (c and d) Li-ZnO. Parts b and d were taken at high magnification, showing the adsorption of dye on the surface of the ZnO aggregates. The sensitization time was 2 h.

Besides the effects of lithium ions on the film morphology (i.e., the polydisperse size distribution of aggregates) and the porosity of aggregates, it was also found that the surface chemistry of ZnO is very different for Li-ZnO and pure-ZnO. It is well-known that ZnO is not stable when it is soaked in acidic dyes because the surface zinc atoms may be dissolved by protons released from the dye molecules.[26,27] This can result in the formation of an inactive Zn^{2+}/dye complex layer on the ZnO surface and, thus, lower the electron injection efficiency from the dye molecules to the ZnO semiconductor. For example, it was reported that the overall conversion efficiency of a DSC based on a ZnO aggregate film tended to gradually decrease when the sensitization time in the N3 dye was longer than 20 min.[38] In the present paper, it is shown that films of pure-ZnO and Li-ZnO are very different with regards to the surface chemistry and that Li-ZnO presents an impressive improvement in the surface stability of ZnO in a ruthenium-based dye solution. This study was performed by soaking the pure-ZnO and Li-ZnO films in the N3 dye for 2 h; such a sensitization time is designed to be at least 6 times longer than the conventional 20−30 min used in the case of ZnO for dye adsorption. These films, after dye sensitization, were characterized by SEM. The results are shown in Figure 8. It is evident that, after suffering an overadsorption of dye, the pure-ZnO film has been covered by a thick layer of complex so that the appearance of an aggregate surface can no longer be clearly observed. Conversely, the Li-ZnO film still displays a relatively distinct nanocrystallite structure with only a very slight accumulation of Zn^{2+}/dye complexes on the aggregate surface. The difference in the dye adsorption for the films of pure-ZnO and Li-ZnO reflects the difference in the surface chemistry of these two films. The Li-ZnO film, which consists of ZnO aggregates synthesized in the presence of lithium ions, indicates an

(35) Fan, Z. Y.; Lu, J. G. Zinc oxide nanostructures: Synthesis and properties. *J. Nanosci. Nanotechnol.* **2005**, *5*(10), 1561–1573.
(36) Ohya, Y.; Saiki, H.; Tanaka, T.; Takahashi, Y. Microstructure of TiO_2 and ZnO films fabricated by the sol−gel method. *J. Am. Ceram. Soc.* **1996**, *79*(4), 825–830.
(37) Fujihara, S.; Sasaki, C.; Kimura, T. Effects of Li and Mg doping on microstructure and properties of sol−gel ZnO thin films. *J. Eur. Ceram. Soc.* **2001**, *21*, 2109–2112.
(38) Chou, T. P.; Zhang, Q. F.; Cao, G. Z. Effects of dye loading conditions on the energy conversion efficiency of ZnO and TiO_2 dye-sensitized solar cells. *J. Phys. Chem. C* **2007**, *111*(50), 18804–18811.

improved surface stability in the ruthenium-based dye. Such an improved surface stability would significantly suppress the formation of a Zn^{2+}/dye complex and, thus, keep the pores of the aggregates from being blocked. This enables a thorough infiltration of dye molecules into the interior of the aggregates and, meanwhile, offers open pathways for electrolyte diffusion within the photoelectrode film when the solar cell is under operating conditions. It is also believed that the improved surface stability favors the attainment of dye adsorption on ZnO in a monolayer, resulting in more effective electron injection at the dye−semiconductor interface.

A possible explanation for the improvement in the surface stability of ZnO in an acidic dye is that the lithium ions may induce the growth of ZnO nanocrystallites by increasing the diffusivity of interstitial zinc atoms, as mentioned above. This would lead to a decrease in the concentration of zinc atoms at the nanocrystallite surface because of the surrounding lithium ions and, thus, likely provide ZnO with an oxygen-enriched surface. Such a surface terminated with enriched oxygen atoms may hinder the reaction between the zinc atoms and the protons released from the dye, therefore suppressing the formation of a Zn^{2+}/dye complex. It should be noted that the existence of an oxygen-enriched surface is just a hypothesis that has been proposed to explain the change in the ZnO surface with respect to dye adsorption. In this study, no difference has been observed in the XPS spectra regarding the oxygen content of pure-ZnO and Li-ZnO.[34] The inability to detect such an oxygen-enriched surface is possibly due to the very small difference in the oxygen content of pure-ZnO and Li-ZnO.

The difference in the dye adsorption for the films of pure-ZnO and Li-ZnO was further explored by a dye-unloading experiment. In this experiment, the films were first sensitized in dye for 20 min and then soaked in a 1 M NaOH water−ethanol (1:1) solution for dye unloading.[39] The solutions with dye desorbed from the films were then characterized by measurement of their UV/visible absorption spectra. The results are shown in Figure 9; an absorption spectrum of a virgin N3 dye solution is also included for reference. It can be seen that all of these dye solutions present three absorption peaks at wavelengths of 310, 375, and 510 nm, corresponding to the characteristic absorption of the N3 dye. The absorption spectra of the solution with dye desorbed from the pure-ZnO film and the solution of virgin N3 dye are almost identical in terms of both their peak positions and relative intensities. However, the solution of dye desorbed from the Li-ZnO film exhibits an absorption that is gradually increased in the near-UV/visible region as the wavelength becomes smaller than 500 nm. It is known that the optical absorption of dye molecules is caused by electron transit from the highest occupied molecular orbital (HOMO) to the lowest unoccupied molecular orbital (LUMO). The N3 dye molecule possesses a structure of four carboxylic groups (COOH) at the end of the pyridyl

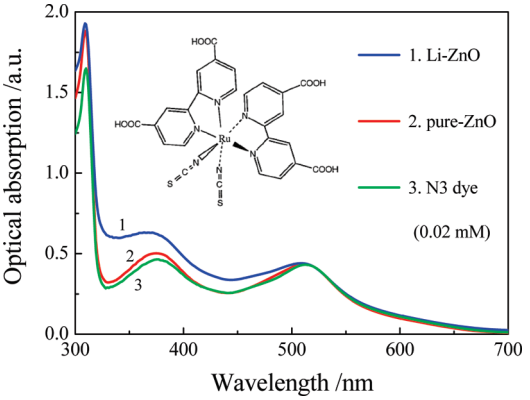

Figure 9. Optical absorption spectra of 0.02 mM N3 dye (···) and solutions with dye unloaded from Li-ZnO (—) and pure-ZnO (- - -) films. The inset is the molecular structure of the N3 dye. The dye adsorption amount is estimated to be about 6.0×10^{-8} mol cm^{-2} for both the pure-ZnO and Li-ZnO films.

rings and two NCS ligands connected to Ru^{II}, as shown in the inset of Figure 9. The HOMO level of the N3 dye is related to the ruthenium metal and NCS ligands, and the LUMO level is associated with the bipyridyl rings and carboxylic groups.[40] In the case of a dye-sensitized oxide semiconductor, the carboxylic groups are spatially close to the semiconductor surface and form a bond with the semiconductor by donating a proton to the oxide lattice.[41] From the results of this study, no evidence was found concerning any change in the molecular structure of the N3 dye after it is desorbed from Li-ZnO. Therefore, the absorption enhancement in the near-UV/visible region, as shown in Figure 9, is not thought to be due to the N3 dye. Considering that the intrinsic absorption of ZnO is at 380 nm, it can be simply inferred that the absorption enhancement may arise from segments of ZnO that have peeled off from the Li-ZnO film and dispersed in the solution. Such a scenario would cause optical absorption in the near-UV/visible region. It is quite interesting that this phenomenon does not occur for pure-ZnO. This likely suggests that the chemical bond between the dye molecules and ZnO is greatly enhanced in the case of Li-ZnO. However, further investigation is ongoing in order to reveal the mechanism of how the lithium ions bond to ZnO and affect the absorption of dye molecules.

A ζ potential analysis was also carried out in order to better understand the lithium-ion-induced change in the surface status of ZnO. The suspension solution was prepared by dispersing pure-ZnO or Li-ZnO aggregates in a solution of ethanol at a concentration of $\sim 1 \times 10^{-3}$ M. The results revealed an obvious difference in the ζ potentials for these aggregates, i.e., an average of 64 ± 2 mV for pure-ZnO and 42 ± 1 mV for Li-ZnO. The ζ potential reflects the interaction between the solid surface and the liquid electrolyte. The ~34% decrease in the ζ potential verified the change in the surface chemistry of ZnO due to the use of a lithium salt during the aggregate synthesis. The results for

(39) Kakiuchi, K.; Hosono, E.; Fujihara, S. Enhanced photoelectrochemical performance of ZnO electrodes sensitized with N-719. *J. Photochem. Photobiol., A* **2006**, *179*(1−2), 81–86.
(40) Gratzel, M. Perspectives for dye-sensitized nanocrystalline solar cells. *Prog. Photovoltaics* **2000**, *8*(1), 171–185.
(41) Hagfeldt, A.; Gratzel, M. Molecular photovoltaics. *Acc. Chem. Res.* **2000**, *33*(5), 269–277.

Table 1. Summary of the Morphology, Structure, Surface Chemistry, and Photovoltaic Properties of pure-ZnO and Li-ZnO Films

sample	dispersivity of aggregates	average crystallite size (nm)	average pore size (nm)	ζ potential (mV)	formation of a Zn^{2+}/dye complex after sensitization	V_{OC}(mV)	I_{SC}(mA cm^{-2})	FF	η (%)[a]
pure-ZnO	mono	10	1.6	64 ± 2	yes	640	13	0.48	4.0
Li-ZnO	poly	12	1.8	42 ± 1	no	660	21	0.44	6.1

[a] $\eta = (V_{OC} I_{SC} \times FF)/P_{in}$, where η is the overall conversion efficiency and P_{in} is the incident power density ($= 100$ mW cm^{-2}).

pure-ZnO and Li-ZnO films with regards to morphology, structure, surface chemistry, and photovoltaic properties are summarized and compared in Table 1. It is evident that the lithium ions exert a significant influence on the growth of ZnO aggregates and result in an improvement in the performance of DSCs.

IV. Conclusions

We have demonstrated that the use of a lithium salt during the synthesis of ZnO aggregates may result in both a polydisperse size distribution of the aggregates and an improvement in the surface stability of ZnO in an acidic dye. The film consisting of as-synthesized Li-ZnO aggregates exhibits a significant increase in the photocurrent density when used in a DSC, and displays a ~53% increase in the overall conversion efficiency. The enhancement in the performance of DSCs with ZnO films consisting of aggregates synthesized in the presence of lithium ions can be ascribed to (1) the polydisperse size distribution of ZnO aggregates, which causes strong light scattering within the photoelectrode film, (2) the increase in the nanocrystallite size of ZnO and the pore size of the aggregates, which offers a more porous structure for dye infiltration and electrolyte diffusion, and (3) the enhanced surface stability of ZnO, which prevents the formation of Zn^{2+}/dye complexes and favors dye adsorption on ZnO in a monolayer. Because of the relatively slight variance in the diffuse-transmittance and -reflectance spectra of the pure-ZnO and Li-ZnO films, as well as the mild change in the pore size distribution of the ZnO aggregates with use of lithium ions for synthesis, factors (1) and (2) were believed to have only a minor impact on the enhancement in the solar cell performance. However, the third factor, an improvement in the surface stability and dye adsorption, was thought to have made the primary contribution to the enhancement in the solar cell performance because an avoidance of the formation of a Zn^{2+}/dye complex in ZnO-based DSCs is especially critical for achieving highly efficient light-harvesting and electron injection from the dye molecules to the semiconductor. Finally, it is worth mentioning that a surface modification like what lithium ions provide in this study is both a simple and feasible approach to increase the surface stability of the ZnO material when used in DSCs. Other cations or anions may also be effective in accomplishing such a modification or possibly lead to a better surface stability. It is anticipated that a resolution of the problem regarding dye adsorption on ZnO may impart the ZnO-based DSCs with power conversion efficiencies much higher than what have reached at present or even comparable to those of TiO_2 (~11%).

Acknowledgment. This work is supported by the U.S. Department of Energy, Office of Basic Energy Sciences, Division of Materials and Engineering under Award No. DE-FG02-07ER46467 (Q.F.Z.), the Air Force Office of Scientific Research (AFOSR-MURI, FA9550-06-1-0326) (K.S.P.), the University of Washington TGIF grant, the Washington Research Foundation, and the Intel Corporation.

Supporting Information Available: XPS characterization of pure-ZnO and Li-ZnO films and the role of lithium ions in the synthesis of ZnO aggregates (PDF). This material is available free of charge via the Internet at http://pubs.acs.org.